INTERNATIONAL JOURNAL FOR NUMERICAL METHODS IN FLUIDS
Int. J. Numer. Meth. Fluids **31**: 1281–1295 (1999)

NUMERICAL PREDICTION OF THE FORMATION OF GOERTLER VORTICES ON A CONCAVE SURFACE WITH SUCTION AND BLOWING

M.H. LIN* AND G.J. HWANG[1]

Department of Power Mechanical Engineering, National Tsing Hua University, Hsinchu 30043, Taiwan, Republic of China

SUMMARY

This paper presents a numerical prediction of the formation of Goertler vortices on a concave surface with suction and blowing. Suction stabilizes the boundary layer flow on the surface, whereas blowing destabilizes the flow. The criterion on the position marking the onset of Goertler vortices is defined in the present paper. For facilitating the numerical study, the computation is carried out in the transformed x–η plane. The results show that the onset position characterized by the Goertler number depends on the local suction/blowing parameter, the Prandtl number and the wavenumber. The value of the critical Goertler number increases with the increase in suction, while the value of the Goertler number decreases with the increase in blowing. Both the experimental and the numerical data can be correlated by $G^*_\theta = 10.2(a'\theta)^{*3/2}$ without suction and blowing and by a simple relation $G^*_x = (G^*_x)_{\gamma=0}\,e^{-\gamma}$ with suction and blowing. The obtained critical Goertler number and wavenumber are in good agreement with the previous experimental data. Copyright © 1999 John Wiley & Sons, Ltd.

KEY WORDS: numerical prediction; Goertler vortices; concave surface; suction and blowing

1. INTRODUCTION

The study of Goertler vortices on a concave wall with the effects of suction and blowing is of practical significance for its engineering applications. The vortex instability is induced by the centrifugal force normal to the surface. This situation is analogous to the occurrence of longitudinal vortices in a boundary layer flow on a heated horizontal flat plate, where a buoyancy force normal to the wall is induced. The studies on the Goertler vortices were reviewed by Herbert [1] and Floryan [2]. Only a few studies on the Goertler vortices with the effect of blowing/suction were performed by Kobayashi [3] and Floryan and Saric [4]. By reviewing the criteria of the onset of the longitudinal vortices in boundary layer and channel flows, the experimental and numerical methods employed in the literature for determining the onset position were summarized in Hwang and Lin [5].

It is noted that the numerical and experimental investigations in the literature on the onset of Goertler vortices with the effect of suction/blowing are rather limited and incomplete. This current study was motivated by a desire to explore the extent of destabilization/stabilization of

* Correspondence to: Department of Automation Engineering, Ta-Hwa Institute of Technology, Hsinchu 307, Taiwan, Republic of China. E-mail: aemhlin@et4.thit.edu.tw
[1] Deceased.

CCC 0271–2091/99/241281–15$17.50

Received June 1998
Revised December 1998

the Blasius flow on a concave surface for the formation of Goertler vortices with the effect of suction/blowing. The experimental criteria proposed by Hwang and Lin [5], marking the onset of longitudinal vortices, were employed in the present study. The Blasius-type basic flow with $X^{-1/2}$ varying suction/blowing model is employed. The governing parameters for the effect of suction/blowing on the onset of Goertler vortices are the Prandtl number, the wavenumber a and the local suction/blowing parameter γ. In the computation, the magnitudes of the applied initial disturbance velocity with an amplitude of $u^0 = 10^{-3}$, and the local blowing/suction parameter $\gamma = 0.5$ to -1.0 are employed.

2. THEORETICAL ANALYSIS

Consider a laminar Blasius flow on a concave wall with a free stream velocity U_∞. As shown in Figure 1, the physical curvilinear co-ordinates are chosen such that X measures the streamwise distance from the leading-edge of the concave wall, Y is the distance normal to the wall, and Z is in the transverse direction. The present study assumes constant fluid thermophysical properties, a large radius of curvature R of a concave wall and a large Reynolds number. The basic flow and energy equations in similarity forms $f''' + ff''/2 = 0$ and $\theta_b'' + Prf\theta_b/2 = 0$ can be found readily in many texts, where $f(\eta) = \psi(vXU_\infty)^{-1/2}$, $\theta_b(\eta) = (T - T_\infty)/(T_w - T_\infty)$ and $\eta = Y(vX/U_\infty)^{-1/2}$. The similarity solutions of the basic quantities will be used to compute the solution of perturbation equations. The Blasius equation can be extended to the case for a small wall velocity, $|V_w| \ll U_\infty$, where V_w is a negative (suction) or positive (blowing) normal velocity. For similarity reasons, only a certain type of $V_w(X)$ is allowed. The wall velocity is $V_w = -f(0)\sqrt{vU_\infty/X}/2$ at $\eta = 0$. Therefore, the wall suction/blowing varying with $X^{-1/2}$ can be simulated by a non-zero value of the Blasius streamfunction f at $\eta = 0$, i.e.

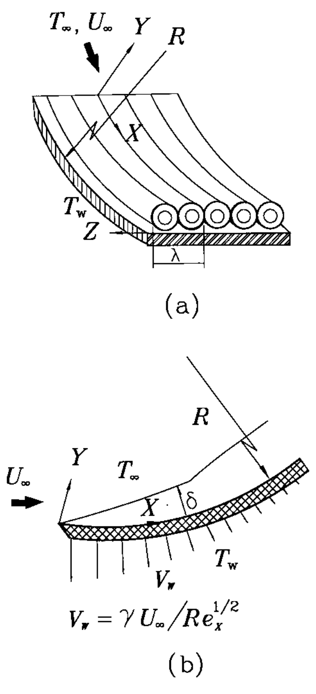

Figure 1. Physical configuration (a) and curvilinear co-ordinate system (b).

$$\gamma = \frac{V_w}{U_\infty} Re_X^{1/2} = -f(0)/2 \quad \text{or} \quad f(0) = -2\gamma. \tag{1}$$

The other boundary conditions are $f'(0) = \theta_b(0) - 1 = f'(\infty) - 1 = \theta_b(\infty) = 0$.

In the region near or upstream of the onset position x^*, the disturbances of longitudinal vortex-type are small and the non-linear terms in the momentum and energy equations may be linearized. Furthermore, in the experiments (Tani [6], Wortmann [7], Bippes [8], Winoto *et al.* [9], Swearingen and Blackwelder [10] and Peerhossaini and Wesfreid [11]), 'stationary' longitudinal vortex rolls have been found periodic with a wavelength λ in the transverse direction Z. Therefore, the disturbances superimposed on the two-dimensional basic flow quantities can be expressed as

$$F(X, Y, Z) = F_b(X, Y) + F'(X, Y)\exp(ia'Z),$$
$$W(X, Y, Z) = w'(X, Y)i\exp(ia'Z), \tag{2}$$

where $F = U$, V, P or T; $f' = u'$, v', p' or t'. $a' = 2\pi/\lambda$ is the dimensional transverse wavenumber of the vortex rolls. By considering the vortex-type perturbation quantities in the continuity equation, a different expression for W is used. Substituting Equation (2) into the continuity, Navier–Stokes and energy equations in curvilinear co-ordinates, and subtracting the two-dimensional basic flow and energy equations under the assumptions of $Re \gg 1$ and $R \gg 1$, one can obtain the linearized perturbation equations.

$$\frac{\partial u'}{\partial x} + \frac{\partial v'}{\partial y} - a'w' = 0, \tag{3}$$

$$U_b\frac{\partial u'}{\partial X} + u'\frac{\partial U_b}{\partial X} + V_b\frac{\partial u'}{\partial Y} + v'\frac{\partial U_b}{\partial Y} = \nu\nabla^2 u', \tag{4}$$

$$U_b\frac{\partial v'}{\partial X} + u'\frac{\partial V_b}{\partial X} + V_b\frac{\partial v'}{\partial Y} + v'\frac{\partial V_b}{\partial Y} = \nu\nabla^2 v' - \frac{1}{\rho}\frac{\partial p'}{\partial Y} - \frac{2}{R}U_b u', \tag{5}$$

$$U_b\frac{\partial w'}{\partial X} + V_b\frac{\partial w'}{\partial Y} = \nu\nabla^2 w' - \frac{1}{\rho}\frac{\partial p'}{\partial Z}, \tag{6}$$

$$U_b\frac{\partial t'}{\partial X} + u'\frac{\partial T_b}{\partial X} + V_b\frac{\partial t'}{\partial Y} + v'\frac{\partial T_b}{\partial Y} = \nabla^2 t', \tag{7}$$

where $\nabla^2 = (\partial^2/\partial Y^2) - a'^2$ is a two-dimensional Laplacian operator. The perturbation equations are two-dimensional and of boundary layer flow type.

Next, one introduces the following dimensionless variables and parameters:

$$X = Rx, \quad [Y \quad Z] = R\,Re^{-1/2}[y \quad z], \quad [U_b \quad u'] = U_\infty[\bar{u} \quad u],$$
$$[V_b \quad v' \quad w'] = U_\infty Re^{-1/2}[\bar{v} \quad v \quad w], \quad [T_b - T_\infty \quad t'] = (T_w - T_\infty)[\theta_b \quad t],$$
$$p' = \frac{\rho U_\infty^2}{Re}p, \quad a' = \frac{Re^{1/2}}{R}a, \quad Re = \frac{U_\infty R}{\nu}, \tag{8}$$

and a vorticity function in the axial direction

$$\xi = \frac{\partial w}{\partial y} - \frac{\partial v}{\partial z} = \frac{\partial w}{\partial y} - av. \tag{9}$$

To obtain an equation for the vorticity, one may differentiate Equations (5) and (6) by z and y respectively, and then eliminate the pressure terms by subtracting one from the other. To derive an equation for v, one may differentiate Equation (9) with respect to z. Similarly, an equation for w can be obtained by differentiating Equation (9) by y. It is noted that, in the derivation of equations for v and w, the continuity equation (3) must be considered. By using also the similarity variable $\eta = y/\sqrt{x}$, the perturbation equations in the η–x plane are found.

$$\frac{\partial^2 u}{\partial \eta^2} + \frac{1}{2} f \frac{\partial u}{\partial \eta} - x f' \frac{\partial u}{\partial x} - a^2 x u + \frac{1}{2} \eta f'' u = f'' \sqrt{x} v, \tag{10}$$

$$\frac{\partial^2 t}{\partial \eta^2} + \frac{1}{2} Pr f \frac{\partial t}{\partial \eta} - x Pr f' \frac{\partial t}{\partial x} - a^2 x t = Pr \frac{\partial \theta_{\mathrm{b}}}{\partial \eta} \left(-\frac{1}{2} \eta u + \sqrt{x} v \right), \tag{11}$$

$$\begin{aligned} &\frac{\partial^2 \xi}{\partial \eta^2} + \frac{1}{2} f \frac{\partial \xi}{\partial \eta} - x f' \frac{\partial \xi}{\partial x} - \left(\frac{1}{2} \eta f'' + a^2 x \right) \xi \\ &= -2 x a Re^{1/2} f' u - a u \left(\frac{1}{4\sqrt{x}} (f - \eta f'' - \eta^2 f''') \right) + \sqrt{x} f'' \left(\frac{\partial w}{\partial x} - \frac{\eta}{2x} \frac{\partial w}{\partial \eta} \right), \end{aligned} \tag{12}$$

$$\frac{\partial^2 v}{\partial \eta^2} - x a^2 v = a x \xi - \sqrt{x} \frac{\partial^2 u}{\partial x\, \partial \eta} + \frac{\eta}{2\sqrt{x}} \frac{\partial^2 u}{\partial \eta^2} + \frac{1}{2\sqrt{x}} \frac{\partial u}{\partial \eta}, \tag{13}$$

$$\frac{\partial^2 w}{\partial \eta^2} - x a^2 w = \sqrt{x} \frac{\partial \xi}{\partial \eta} - a x \frac{\partial u}{\partial \eta} + \frac{1}{2} a \eta \frac{\partial u}{\partial \eta}. \tag{14}$$

The above equations are in the x–η plane instead of the x–y plane. The η-axis covers all the variations of the main flow in the x–y plane and probably covers most of the variation of perturbation quantities. Therefore, the computer time for solving Equations (10)–(14) may be much shorter than that for equations in the x–y plane. The set of Equations (5)–(9) is a boundary value problem in the η-direction, an initial value problem in the x-direction, and an eigenvalue problem in the z-direction. This type of formulation and approach completely abandons the conventional approach in seeking an undefined solution with a fixed zero or other finite values of x derivatives. The growth of magnitude of longitudinal vortices is part of the solution. The appropriate initial condition and boundary conditions of the perturbations equations are

$$\begin{aligned} &u = v = w = t = 0 && \text{at } \eta = 0, \\ &u = v = w = t = \xi = 0 && \text{at } \eta = 0, \\ &u - u^0 = v = w = \xi = t = 0 && \text{at } x = 0. \end{aligned} \tag{15}$$

For simplicity, the initial amplitude function u^0 is set uniform, and the other two velocity components v and w are set to zero. However, the magnitudes of the velocities v and w will be generated in the next x steps. The range of the initial amplitude function, $u^0 = 10^{-3}$ is used in the present study. In the experiment of Swearingen and Blackwelder [10], the free stream turbulence level in their well-controlled wind tunnel was less than 0.07%, corresponding to the perturbation velocity u with a magnitude between 10^{-4} and 10^{-3}.

Equations (10)–(14) and boundary conditions (15) in the x–η plane are for unknowns u, t, ξ, v and w with two fixed values of a and Re. By giving a series value of a, the largest amplification of the perturbation quantities along the x-direction determines the value of critical wavenumber a^*. One can see that the term $-2xaRe^{1/2}f'u$ on the right-hand side of Equation (12) may be expressed as $-2(x^{1/2}a)(xRe)^{1/2}f'u$, in which $(x^{1/2}a)$ is the dimensionless wavenumber defined by using the local boundary layer thickness, and $xRe = U_\infty X/v$ is the local Reynolds number. The radius of curvature does not appear explicitly in Equations (10)–(14). One may prove analytically the homogeneity of R in Equations (10)–(14) by considering the dimensionless transformations (8), i.e. $v \sim R^{1/2}$, $w \sim R^{1/2}$, $x \sim R^{1/2}$, $y \sim R^{1/2}$,

$z \sim R^{1/2}$ and $\xi \sim R$ (variables of u, η and f are independent of R). In the computation, the selection of Re does not change the local critical Reynolds number $(xRe)^*$ and the critical wavenumber $(x^{1/2}a)^*$. This is also proved by using several values of Re in the computation. For the present study, $Re^{1/2} = 250$ is used for demonstrating the results.

The local friction factor and the local Nusselt number of the basic and perturbed flows can be also expressed respectively as

$$C_{fX} = C_{f\mathrm{b}} + C_{f\mathrm{p}} = \frac{\tau_{\mathrm{wb}} + \tau_{\mathrm{wp}}}{\frac{1}{2}\rho U_\infty^2} = 2\, Re_X^{-1/2}\left[f''(0) + \left.\frac{\partial u}{\partial \eta}\right|_{\mathrm{w}} \right], \tag{16}$$

$$Nu_X = Nu_{\mathrm{b}} + Nu_{\mathrm{p}} = \frac{(h_{\mathrm{b}} + h_{\mathrm{p}})X}{k} = -Re_X^{-1/2}\left[\theta'_{\mathrm{b}}(0) + \left.\frac{\partial t}{\partial \eta}\right|_{\mathrm{w}} \right], \tag{17}$$

where τ_{w} and h are the local wall shear stress and local heat transfer coefficient respectively; the subscripts b and p indicate the basic and perturbed flows, and k is the fluid thermal conductivity. It is noted that the Nu_X is based on the thermal boundary condition of constant wall temperature.

3. NUMERICAL PROCEDURE

A finite difference scheme based on the weighting function of Lee [12] with second-order accuracy in both η and x is used. The step-by-step procedure is listed as follows:

1. Assign Pr and γ to obtain the basic flow and temperature distributions. The value of Pr is 0.7 and the values of γ are 0, ± 0.2 ± 0.3 ± 0.4, ± 0.5 and -1.0 in the present study.
2. Assign $Re^{1/2} = 250$, zero initial values of v, w, ξ and t, initial velocity at the leading-edge, $u^0 = 10^{-3}$ and various values of wavenumber a.
3. Solve Equations (10)–(12) for u, t and ξ distributions at the next x step. Values of ξ on the boundary are evaluated with previous iteration data of v and w in the interior region.
4. Solve Equations (13) and (14) for v and w with the obtained u and ξ.
5. Repeat steps 3 and 4, until the perturbation quantities meet the convergence criteria at the streamwise position

   $$\mathrm{Max}\left(\frac{|F_{i,j}^{(n+1)}| - |F_{i,j}^{(n)}|}{|F_{i,j}^{(n+1)}|} \right) \leq 10^{-5},$$

   where $F_{i,j}^{(n)}$ are the perturbation quantities u, v, w, t and ξ of nodal point (i, j) at the nth iteration.
6. Calculate the local friction factor and the local Nusselt number of the vortex flow.
7. Repeat steps 3–6 at the next mainstream position until a desired mainstream position is reached.
8. The absolute values of perturbation quantities are growing along the mainstream direction. One can find the mainstream position marked with the subscript i, where the flow visualization onset criterion $Y_i = \int_0^{X^*} \mathrm{Max}|v'|(\mathrm{d}X/U_\infty) = 2$ mm or $y_i = \int_0^{x^*} \mathrm{Max}_j\, |v_{i,j}^{(n)}|\, \mathrm{d}x = 0.002$ is satisfied, where Y_i is the detectable height of the vortex spike. Various onset positions x_{cr} can be determined for different values of wavenumber a. The minimum x_{cr}, denoted by x^*, is the most probable onset position and the corresponding wavenumber is denoted by a^*. The local critical Goertler number is $G_x^* = 2x^*Re^{1/2}$ and the local wavenumber is $a^*x^{*1/2}$ for this computation.

Table I. Grid size test for $Re^{1/2}=250$, $a^*=1.34$, $Pr=0.7$ and $\gamma=0$

Δx	$\Delta\eta$	x				
		0.1	0.2	0.3	0.4	0.5
0.002	0.02	0.01437[a]	0.04952	0.2413	1.733	16.05
0.002	0.01	0.01437	0.04952	0.2412	1.732	16.04
0.001	0.02	0.01431	0.04942	0.2408	1.730	16.02

[a] These are the maximum values of the mainstream velocity $u/0.01$ at the specified x position.

The grids tested for various Δx and $\Delta\eta$ are listed in Table I. A grid size of $\Delta x=0.002$, $\Delta\eta=0.02$ and $\eta_\infty=10$ is used to perform the numerical experiment in this study. To check the validity of the linear Equations (10)–(14), the order of magnitude of non-linear terms of perturbation equations near the onset position are checked. The calculated data are substituted into the individual terms of the x momentum equation. The orders of the non-linear terms is two orders of magnitude smaller than the order of linearized inertia terms. Therefore, the linear theory is valid for the estimation of the onset of Goertler vortices.

4. RESULTS AND DISCUSSION

The typical development of the dimensionless perturbation amplitudes u, v, w and t at $x=0.35$, 0.4, 0.45 and 0.5 for $Pr=0.7$, $Re^{1/2}=250$, $a^*=1.34$ and $\gamma=0$ is shown in Figure 2. The magnitudes of v and w are larger than those of u and t because the scaling factor $Re^{-1/2}$ is included in these quantities. As shown in Equation (2), the profiles for u, v and t correspond to the perturbation amplitude along $z=0$ only, while the profile for w is along $z=\pi/2a$. The transverse perturbation velocity amplitude w behaves like a sine function in the η-direction. Along $z=0$, the negative perturbation velocity v causes a negative perturbation temperature t and a positive perturbation velocity u. The shapes of the v and w profiles may be regarded as a vortex pattern. This figure also presents the development of the perturbation amplitude quantities in the streamwise direction. It is seen that the perturbation amplitude quantities are very small at $x\leq 0.35$, and increase rapidly along the streamwise direction at $x\geq 0.4$.

Figure 3 depicts the dimensionless perturbation amplitude functions at $x=0.3$, 0.35 and 0.4, with wall suction $\gamma=-0.5$. It is seen that the values of perturbation amplitude functions are decreased with the stabilizing effect of a negative γ. It is also observed in this figure that the profiles of the perturbation amplitude functions are shrunk to a smaller η region due to the suction effect. In contrast, as shown in Figure 4, the values of the perturbation function are increased, and the sizes of the function are enlarged to a larger η region with a positive γ.

The variations of velocity boundary layer thickness $\delta Re_X^{1/2}/X$ with the parameter G_x are shown in Figure 5. One obtains G_x by using $G_x=2(X/R)Re_X^{1/2}=2x^{3/2}Re^{1/2}$. The local Goertler number G_x is varying with $x^{3/2}$ along the mainstream direction. It is seen that $\delta Re_X^{1/2}/X=5.0$ is for zero blowing and suction, $\delta Re_X^{1/2}/X>5.0$ is for blowing, and $\delta Re_X^{1/2}/X<5.0$ is for suction. It is noted that the onset of vortices in the boundary layer is not associated with any immediate increase in the thickness of the boundary layer. However, further downstream from the onset point, a sharp increase in the boundary layer thickness is observed. A similar trend is also observed in experiments by Swearingen and Blackwelder [10]. The turbulent boundary layer thickness based on the one-seventh power-law velocity profile for a flat plate (White [13])

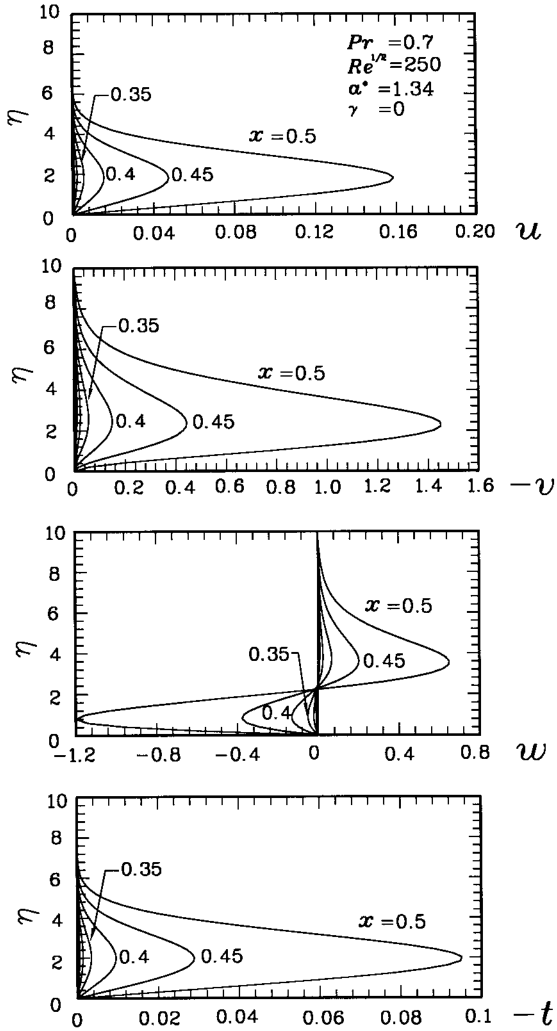

Figure 2. Development of the perturbation amplitude profiles at specified x positions for $\gamma = 0$ ($Pr = 0.7$, $Re^{1/2} = 250$ and $a^* = 1.34$).

$$\delta/X \approx 0.16 Re_X^{-1/7} \quad \text{or} \quad \delta Re_X^{1/2}/X \approx 0.16 Re_X^{5/14} = 0.16[(G_X\, Re/2)^{2/3}]^{5/14}, \tag{18}$$

is also shown for comparison. The boundary layer thickness is thicker, and thus the flow is more unstable when the effect of blowing is applied, and *vice versa*. It is noted that the theory predicts a smaller boundary layer growth rate than that of Swearingen and Blackwelder [10]. This may be because of the elimination of the non-linear terms and the interaction between the flows inside and outside of the boundary layer.

It is also interesting to study numerically the variations of friction factor and heat transfer coefficient after the onset of Goertler vortices. The variations of local $C_{fX} = C_{fb} + C_{fp}$ and $Nu_X = Nu_b + Nu_p$ along the axial direction at $z = 0$ are shown in Figure 6(a) and (b) respectively. The friction factor coefficient for the turbulent boundary layer flow based on the one-seventh power-law velocity profile (White [13]) is

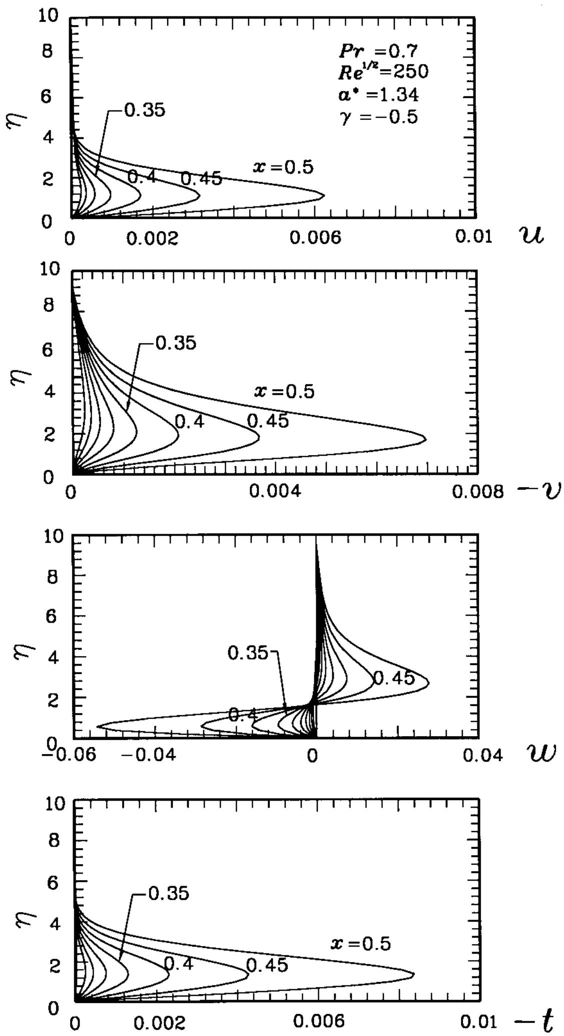

Figure 3. Development of the perturbation amplitude profiles at specified x positions for $\gamma = -0.5$ ($Pr = 0.7$, $Re^{1/2} = 250$ and $a^* = 1.34$).

$$C_{fX} \approx 0.027 Re_X^{-1/7} \quad \text{or} \quad C_{fX} Re^{1/2} \approx 0.027 Re_X^{5/14} = 0.027[(G_X Re/2)^{2/3}]^{5/14}, \tag{19}$$

and the correlation equation for turbulent forced convection (Bejan [14]) is

$$Nu_X = 0.0296 Re_X^{4/5} Pr^{1/3} \quad \text{or}$$

$$Nu_X Pr_X^{-1/2} Re_X^{1/2} = 0.0296 Re_X^{3/10} = 0.0296[(G_X Re/2)^{2/3}]^{3/10}. \tag{20}$$

The friction factor and the Nusselt number are also shown for comparison. The gradients of the velocity and the temperature at the wall start to deviate from the laminar forced convection downstream of x^*. This is due to the secondary longitudinal vortex flow on the heated concave wall. The effects of suction/blowing on Goertler vortices are more pronounced when the values of local suction/blowing parameter γ are decreased/increased. The critical values of G_X^* and the local critical wavenumber $a^* x^{*1/2}$ may be converted to G_θ^* and $a'^*\theta$ respectively by the following transformations:

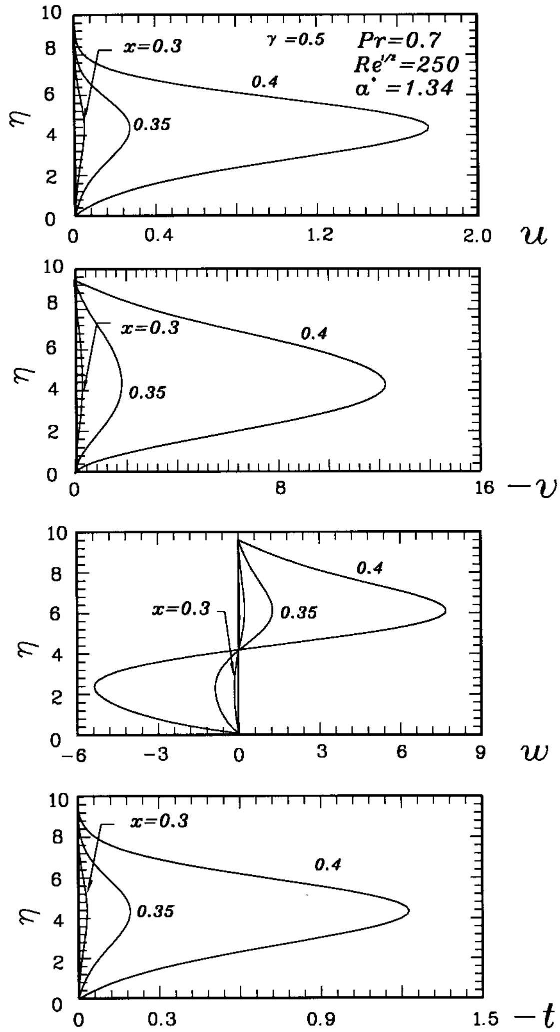

Figure 4. Development of perturbation amplitude profiles at specified x positions for $\gamma = 0.5$ ($Pr = 0.7$, $Re^{1/2} = 250$ and $a^* = 1.34$).

$$G_\theta^* = \frac{U_\infty \theta}{\nu}\sqrt{\frac{\theta}{R}} = [(0.664)^3 G_X^*/2]^{1/2} \quad \text{and} \quad (a'\theta)^* = \left(\frac{2\pi}{\lambda}\frac{0.664X}{Re_X^{1/2}}\right)^* = 0.664(ax^{1/2})^*, \tag{21}$$

where the momentum thickness $\theta = 0.664X/Re_X^{1/2}$. Furthermore, by eliminating the momentum thickness θ between the parameter G_θ and the wavenumber $a'\theta$, we may obtain the relation

$$\frac{G_\theta}{(a'\theta)^{3/2}} = U_\infty \nu^{-1} R^{-1/2}(a')^{-3/2} = Re^{1/4}/a^{3/2} = K \quad \text{or} \quad G_\theta = K(a'\theta)^{3/2}. \tag{22}$$

Experimental results (Tani [6], Wortmann [7], Bippes [8], Winoto *et al.* [9], Winoto and Crane [15], Swearingen and Blackwelder [10] and Peerhossaini and Wesfreid [11], etc.) indicate that the wavelengths of the longitudinal vortices are kept constant in the downstream of onset positions. The growth of the vortices with constant wavelength can be shown by straight lines of gradient $\frac{3}{2}$ on a logarithmic scale in Figure 4 of Tani [6]. It is noted that the value K can be

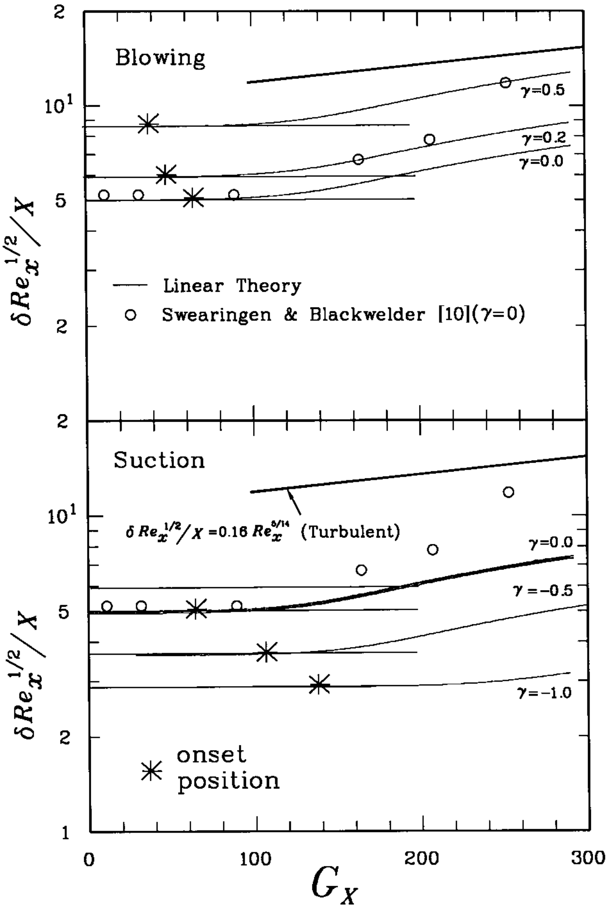

Figure 5. Development of boundary layer thickness.

determined by the assigned Re, and the obtained wave number a. For $Re^{1/2}=250$ and $a=1.34$, $K=10.2$ is calculated.

As shown in Figure 7 of Hall [16], the theoretical critical wavenumber is seen to be three times larger than that from the experimental data of Tani [6]. By considering Equation (22) and keeping constant G_θ^*, one may modify the data of $(a'\theta)$ in experiments by the following transformations:

$$(a'\theta)_{\mathrm{mod}}=\frac{(a'\theta)_{\mathrm{r}}}{(a'\theta)_{\mathrm{exp}}}(a'\theta)_{\mathrm{exp}}=\left(\frac{\lambda_{\mathrm{exp}}}{\lambda_{\mathrm{r}}}\right)\left(\frac{v_{\mathrm{r}}}{v_{\mathrm{exp}}}\right)^{2/3}\left(\frac{U_{\mathrm{exp}}}{U_{\mathrm{r}}}\right)^{2/3}\left(\frac{R_{\mathrm{r}}}{R_{\mathrm{exp}}}\right)^{1/3}(a'^*\theta)_{\mathrm{exp}}\quad\text{or}$$

$$(a'\theta)_{\mathrm{mod}}=\left(\frac{Re_{\mathrm{exp}}}{Re_{\mathrm{r}}}\right)^{1/6}\frac{a_{\mathrm{r}}}{a_{\mathrm{exp}}}(a'\theta)_{\mathrm{exp}},\tag{23}$$

where the subscripts mod, r and exp denote modified, reference and experimental conditions respectively. For example, $U_{\mathrm{r}}=1\ \mathrm{m\,s^{-1}}$, $R_{\mathrm{r}}=1$ m, $v_{\mathrm{r}}=1.56\times10^{-5}\ \mathrm{m^2\,s^{-1}}$ (air at 20°C and atmospheric pressure), and $\lambda_{\mathrm{r}}=1.85$ cm, are set in the present study. Figure 7 summarizes the results of the present and the previous works for the onset of longitudinal vortices on a concave wall. It is seen that there is at least one order of magnitude difference between

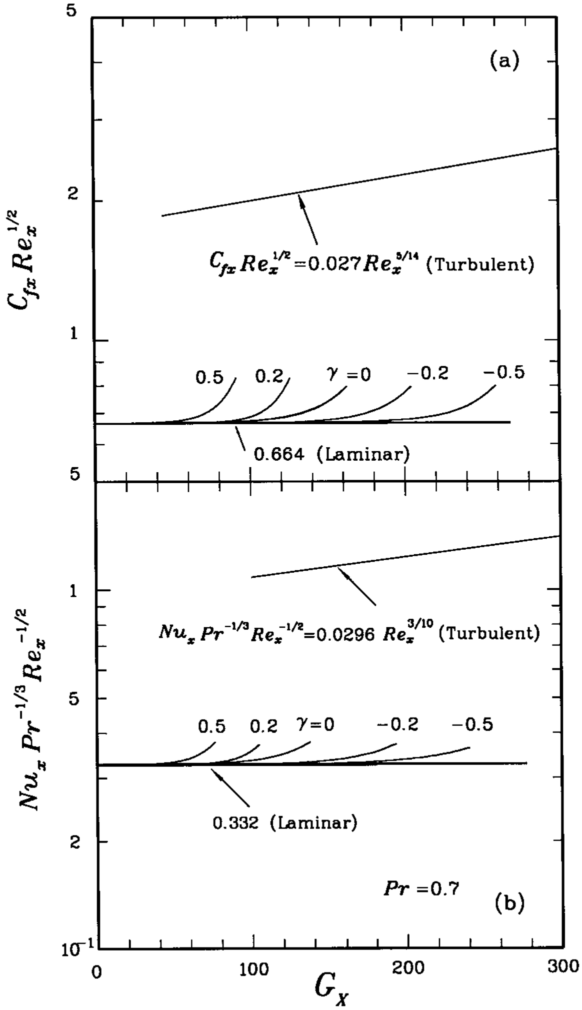

Figure 6. Friction factor and Nusselt number for $\gamma = 0$, ± 0.2 and ± 0.5.

experimental data of the critical Goertler number and those of the theoretical predictions by using zero x derivative (Goertler [17], Smith [18], Floryan and Saric [19], etc.). However, Hall [16] used the criterion of energy method on a concave wall by considering x-dependence derivatives terms. The results of the critical Goertler number predicted by the present study are close to the experimental data. Furthermore, by using the modified $(a'\theta)_{\text{mod}}$, all the experimental data, including two air data and two water data, and covering the range of $U_{\text{exp}} = 0.0325$–16 m s^{-1} and $R_{\text{exp}} = 0.11$–10 m are correlated by the theoretical relation $G_\theta^* = 10.2(a'\theta)^{*3/2}$ to within an error of $\pm 10\%$.

The effect of the suction/blowing parameter γ on the critical Goertler number G_X^* is listed in Table II. It is observed from the data that an increase in the suction rate γ from 0 to -1.0 is to increase up to 2.5 times the value of the critical Goertler number G_X^*. While an increase in the blowing rate γ from 0 to 0.5 is to decrease G_X^* by 0.56 times. The numerical results can be correlated by a simple relation $G_X^* = (G_X^*)_{\gamma=0}\,\mathrm{e}^{-\gamma}$, as shown in Figure 8.

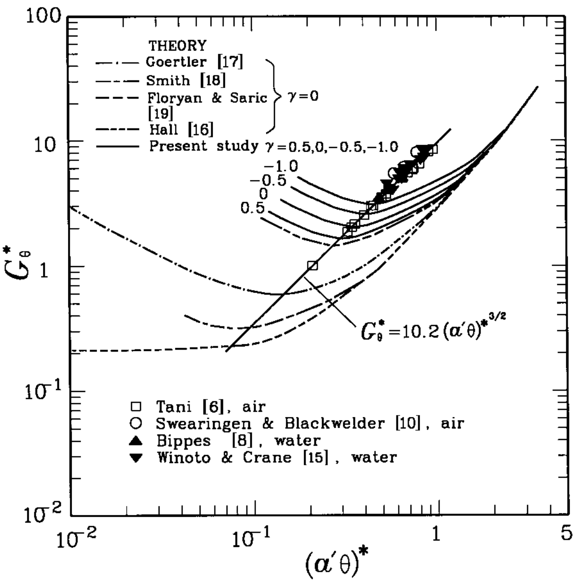

Figure 7. The relation between the critical values G^*_θ and wave number $a'^*\theta$.

In the above analysis, three sets of parameters are used. The three sets of parameters are summarized and discussed as follows. First of all, x^* and a^* are sought by using fixed *Pr* and *Re*. Secondly, x^* and a^* are converted to G^*_X and $a^*x^{*1/2}$. Finally, G^*_θ and $(a'\theta)^*$ are used. The first set of parameters, mainly comes from the length-scale of radius of curvature. The second set of parameters considers the centrifugal force to viscous force ratio and boundary layer thickness. The third set of parameters is derived from the momentum thickness.

5. CONCLUSIONS

(1) The effects of blowing and suction on the destabilization and stabilization of the Blasius flow on a concave surface for the formation of Goertler vortices are studied numerically by using an experimental criterion and an $x^{-1/2}$ varying blowing and suction model.

Table II. Onset position x^* for the criterion $y_i = \int_0^{X^*} \mathrm{Max}_j \, |v_{i,j}^{(n)}| \, \mathrm{d}x = 0.002$

γ	x^*	G^*_X	$a^*x^{*1/2}$
0.5	0.110	18.2	0.444
0.4	0.116	19.8	0.456
0.3	0.124	21.8	0.472
0.2	0.134	24.5	0.491
0.0	0.162	32.6	0.539
−0.2	0.179	38.0	0.567
−0.3	0.192	42.0	0.587
−0.5	0.218	51.0	0.626
−1.0	0.301	82.0	0.735

These values are evaluated by using $Re^{1/2} = 250$, $a^* = 1.34$, $Pr = 0.7$ and $u^0 = 10^{-3}$.

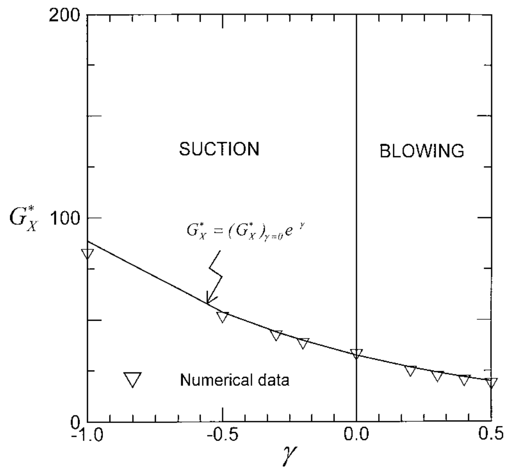

Figure 8. Correlation of theoretical values of G_X^*.

(2) An increase in the suction rate γ from 0 to -1.0 is to increase, by up to 2.5 times, the value of the critical Goertler number G_X^*, while an increase in the blowing rate γ from 0 to 0.5 is to decrease G_X^* by 0.56 times. Both the experimental and numerical data can be also correlated by $G_\theta^* = 10.2(a'\theta)^{*3/2}$ for $\gamma = 0$ and by a simple relation $G_X^* = (G_X^*)_{\gamma=0}\,e^{-\gamma}$ for $\gamma \neq 0$.
(3) The effect of boundary layer growth, the friction factor and the Nusselt number with the γ are also examined. The onset of vortices in the boundary layer flow is not associated with an immediate increase in the rate of boundary layer growth, local friction factor and Nusselt number. However, further downstream from the onset point, a sharp increase is observed. Thus, the boundary layer thickness, friction factor and Nusselt number are less sensitive to the onset of longitudinal vortices.

ACKNOWLEDGMENTS

M.H. Lin wishes to express his appreciation to the National Science Council, Taiwan (Grant No. NSC85-2212-E007-026), for their encouragement and financial support of this work. This paper is dedicated to Professor G.J. Hwang, who died after completion of the work.

APPENDIX A. NOMENCLATURE

a', a	dimensional and dimensionless wavenumber, $a' = aRe^{1/2}/R$
C_f	friction factor, $2\tau_w/\rho U_\infty^2$
f	reduced streamfunction, $\psi(\nu X U_\infty)^{-1/2}$
F	velocity, pressure or temperature function
G_X	local Goertler number, $2XRe_X^{1/2}/R$
h	local heat transfer coefficient
p', p	dimensional and dimensionless pressure, $p' = \rho U_\infty^2 p/Re$
Pr	Prandtl number, ν/α
Nu_X	local Nusselt number, hX/k

R	radius of curvature (m)
Re	Reynolds number based on radius of curvature, $U_\infty R/\nu$
Re_X	local Reynolds number, $U_\infty X/\nu$
T	temperature (K)
t', t	dimensional and dimensionless perturbation temperature, $t' = (T_w - T_\infty)t$
U, V, W	dimensional velocity components (m s^{-1})
u, v, w	dimensionless perturbation velocity components
u', v', w'	perturbation velocity components
u^0	initial constant perturbation velocity at $x = 0$
X, Y, Z	Cartesian co-ordinates (m)
x, y, z	dimensionless Cartesian co-ordinates as defined in (8)

Greek letters

δ	boundary layer thickness (m)
ψ	streamfunction (m^2 s^{-1})
γ	local suction/blowing parameter, $V_w Re_X^{1/2}/U_\infty$
η	Blasius similarity variable, $Y/(\nu X/U_\infty)^{1/2}$
λ	wavelength in Z-direction (m)
ν	kinematic viscosity of fluid (m^2 s^{-1})
θ	momentum thickness, $0.664X/Re_X^{1/2}$
θ_b	dimensionless basic temperature, $(T - T_\infty)/(T_w - T_\infty)$
τ	local wall stress
ξ	vorticity function in the X-direction defined in (9) (s^{-1})

Superscripts

*	onset position

Subscripts

b	basic flow quantity
exp	experimental value
p	perturbation quantity
r	reference
w	wall condition
X	local co-ordinate
θ	momentum thickness
∞	free stream condition
mod	modified value

REFERENCES

1. T. Herbert, 'On the stability of boundary layer along a concave wall', *Arch. Mech.*, **28**, 1039–1055 (1976).
2. J.M. Floryan, 'On the Goertler instability of boundary layers', *Prog. Aerosp. Sci.*, **28**, 235–271 (1991).
3. K. Kobayashi, 'Note on the stability of a boundary layer on a concave wall with suction', *J: Fluid Mech.*, **52**, 269–272 (1972).
4. J.M. Floryan and W.S. Saric, 'Effect of suction on the Goertler instability of boundary layers', *AIAA J.*, **21**, 1635–1639 (1983).

5. G.J. Hwang and M.H. Lin, 'Estimation of the onset of longitudinal vortices in a laminar boundary layer heated from below', *ASME J. Heat Transf.*, **117**, 835–842 (1995).
6. I. Tani, 'Production of longitudinal vortices in the boundary layer along a concave wall', *J. Geophys. Res.*, **67**, 3075–3080 (1962).
7. F.X. Wortmann, 'Visualization of transition', *J. Fluid Mech.*, **38**, 473–480 (1969).
8. H. Bippes, 'Experimental study of the laminar–turbulent transition of a concave wall in a parallel flow', *NASA*, *TM-75243*, 1978.
9. S.H. Winoto, D.F.G. Durao and R.I. Crane, 'Measurements within Goertler vortices', *ASME J. Fluids Eng.*, **101**, 517–520 (1979).
10. J.D. Swearingen and R.F. Blackwelder, 'The growth and breakdown of streamwise vortices in the presence of a wall', *J. Fluid Mech.*, **182**, 255–290 (1987).
11. H. Peerhossaini and J.E. Wesfreid, 'On the inner structure of streamwise Goertler rolls', *Int. J Heat Fluid Flow*, **9**, 12–18 (1988).
12. S.L. Lee, 'Weighting function scheme and its application on multidimensional conservation equations', *Int. J. Heat Mass Transf.*, **32**, 2065–2073 (1989).
13. F.M. White, *Viscous Fluid Flow*, 2nd edn., McGraw-Hill, New York, 1991.
14. A. Bejan, *Heat Transfer*, 1st edn., Wiley, New York, 1993.
15. S.H. Winoto and R.I. Crane, 'Vortex structure in laminar layers on a concave wall', *Int. J. Heat Fluid Flow*, **2**, 221–231 (1980).
16. P. Hall, 'The linear development of Goertler vortices in growing boundary layers', *J. Fluid Mech.*, **130**, 41–58 (1983).
17. H. Goertler, 'Instabilitat Laminarer Grenzchichten an Konkaven wanden Gengenuber Gewissen Deeidimensionalen Storungen', *ZAMM*, **21**, 250–252 (1941).
18. A.M.O. Smith, 'On the growth of Taylor–Goertler vortices along highly concave walls', *Q. J. Appl. Math.*, **13**, 233–262 (1955).
19. J.M. Floryan and W.S. Saric, 'Stability of Goertler vortices in boundary layers', *AIAA J.*, **20**, 316–324 (1982).

